Food Chemistry 203 (2016) 505–512

Contents lists available at ScienceDirect

Food Chemistry

journal homepage: www.elsevier.com/locate/foodchem

Citrinin mycotoxin recognition and removal by naked magnetic nanoparticles

Massimiliano Magro [a,b], Denise Esteves Moritz [c], Emanuela Bonaiuto [a], Davide Baratella [a], Milo Terzo [a], Petr Jakubec [b], Ondřej Malina [b], Klára Čépe [b], Glaucia Maria Falcao de Aragao [c], Radek Zboril [b], Fabio Vianello [a,b,*]

[a] Department of Comparative Biomedicine and Food Science, University of Padua, Italy
[b] Regional Centre of Advanced Technologies and Materials, Department of Physical Chemistry, Palacký University in Olomouc, Czech Republic
[c] Department of Chemical and Food Engineering, Campus Reitor João David Ferreira, Federal University of Santa Catarina (UFSC), Florianópolis (SC), Brazil

ARTICLE INFO

Article history:
Received 17 September 2015
Received in revised form 12 December 2015
Accepted 30 January 2016
Available online 17 February 2016

Keywords:
Food safety
Monascus
Citrinin
Magnetic nanoparticles
Mycotoxin removal
Natural dyes

ABSTRACT

Citrinin is a nephrotoxic mycotoxin which can be synthesized by *Monascus* mold during the fermentation process in foods. *Monascus*, generally described as red mold, is a red-pigmented filamentous fungus attracting a great interest for the production of natural dyes and cholesterol-lowering statins. We individuated a specie of *Monascus* producing high amount of natural dyes. However, this high pigmentation was correlated with the production of citrinin. Peculiar magnetic nanoparticles, synthesized in-house and called "Surface Active Maghemite Nanoparticles" (SAMNs), are proposed as an efficient and reliable mean for citrinin removal from *Monascus* treated foods. The nanomaterial efficiency for citrinin binding was proved on *Monascus* suspensions, and SAMN@citrinin complex was characterized by Mössbauer spectroscopy and magnetization measurements, showing that SAMNs resulted structurally and magnetically well conserved after citrinin binding. SAMNs are excellent and stable magnetic nano-carrier for toxin removal, which can be applied in food industry.

1. Introduction

Currently about 70% of colorants employed in processed foods are ordinary chemical dyes. In the past decades natural dyes lost market, as synthetic chemicals have better consistency and stability, greater range of colors and lower cost. Notwithstanding, in recent years consumer concern pressed for increasing the use of natural dyes obtained from plants and microorganisms. Natural dyes are commonly used for foods, such as meat, sweets, fruit juices, etc., and in the pharmaceutical field, mainly in the encapsulation of active ingredients. In 2007, the market of natural dyes was estimated around 1.15 billion dollars and, according to Leatherhead Food International, since 2004, it has risen of about 2.5% per year (Mapari, Thrane, & Mey, 2010).

Fungi from the *Monascus* genus are a promising source for natural color additives. *Monascus*, also known as red mold, produces at least six different pigments (Meinicke et al., 2012), and more than 50 patents are available about dye production by *Monascus* (Hajjaj, François, Goma, & Blanc, 2012), indicating the great technological interest aroused about this fungus as a source of natural dyes. Furthermore, discoveries of cholesterol-lowering statins produced by *Monascus* have prompted research into its possible medical uses. Notwithstanding, depending on growing conditions, *Monascus* can produce a mycotoxin, citrinin ((*3R,4S*)-8-hydroxy-3,4,5-trimethyl-6-oxo-4,6-dihydro-*3H*-isochromene-7-carboxylic acid), which is also produced by several species of the genera *Aspergillus* and *Penicillium* (EFSA, 2012), with risks for public and animal health, related to its presence in food and feed. Generally, citrinin is formed in plants after harvest, and occurs mainly in stored grains, but also in other products, such as beans, fruits, herbs and spices, and also in spoiled dairy products (Da Lozzo, Mangrich, Rocha, De Oliveira, & Carnieri, 2002). Citrinin control and detection in foods appears very relevant for food safety, as citrinin is nephrotoxic, and may cause serious health problems (Xu, Jia, Gu, & Sung, 2006). This mycotoxin was correlated to a decrease in the cellular ATP content and to an increase of the generation of reactive oxygen species in cells (Da Lozzo, Oliveira, & Carnieri, 1998; Da Lozzo et al., 2002; Hoehler, Marquardt, McIntosh, & Xiao, 1996; Ribeiro, Campello, Chagas, & Kluppel, 1998; Ribeiro,

* Corresponding author at: Department of Comparative Biomedicine and Food Science, University of Padua, Agripolis – Viale dell'Università 16, Legnaro 35020 (PD), Italy.
E-mail address: fabio.vianello@unipd.it (F. Vianello).

http://dx.doi.org/10.1016/j.foodchem.2016.01.147
0308-8146/

Chagas, Campello, & Kluppel, 1997; Stormer & Hoiby, 1996). Thus, its removal from fermentation broths and foods is an attractive task for health, environmental and economic reasons (Da Lozzo et al., 2002).

Ideally, foods fermented by *Monascus* should involve the selection of strains producing large amount of bio-pigments, but, obviously, no citrinin.

Food industry is slowly accepting nanotechnologies, and this is not surprising as public preference for "natural" food products has historically inhibited the implementation of emerging technologies in food processing. Indeed, while public opinion about nanotechnology applications has ranged from neutral to slightly positive (Currall, King, Lane, Madera, & Turner, 2006; Satterfield, Kandlikar, Beaudrie, Conti, & Harthorn, 2009), recent studies suggested that consumers remain wary about "nanofoods" (International Risk Governance Council, 2009; Siegrist, Keller, Kastenholz, Frey, & Wiek, 2007). Nevertheless, scientists and industry stakeholders have already identified potential uses of nanotechnology in virtually every segment of food industry, from agriculture to food packaging, nutrient supplementation and, of course, food processing.

One of the main drawbacks drastically limiting the exploitation of nanoparticles at industrial level is attributable to the difficulty of moving from laboratory to large scale production. Often the synthesis of nanomaterials involves impressive consumption of solvents, high costs and heavy impact on the environment. Thus, to be really taken into consideration, nanoparticles should be produced by a protocol responding to specific requirements, such as cost effectiveness and environmental friendliness. In particular, generally, magnetic nanoparticles need to be stabilized to avoid aggregation and to guarantee long-term stability, pH and electrolyte tolerance, and proper surface chemistry. Nanoparticle coating processes are often cumbersome, time-consuming, and expensive, with low yields, limiting their massive application. By this point of view, novel magnetic nanoparticles, called SAMNs (Surface Active Maghemite Nanoparticles) represent an ideal material, as their synthetic protocol is suitable for being scaled up to an industrial level and is carried out in water, without the employment of any organic solvent (Magro, Valle, Russo, Nodari, & Vianello, 2012). SAMNs represent a new class of naked superparamagnetic maghemite nanoparticles, constituted of stoichiometric maghemite (γ-Fe_2O_3) in the dimension range around 10 nm (Magro et al., 2012). Moreover, SAMNs are stable in water for several months as colloidal suspensions without any superficial modification or coating derivatization, displaying the ability to selectively bind several biomolecules (Magro et al., 2014; Magro and Baratella et al., 2014; Magro et al., 2015; Sinigaglia et al., 2012; Venerando et al., 2013).

Chelating properties of citrinin toward iron(III) were already reported in literature (Da Lozzo et al., 2002). Thus, the availability of iron(III) atoms on the surface of SAMNs was exploited for the recognition and magnetically removal of citrinin from *Monascus* in biological matrixes. In the current report, we present a promising nanoparticle application for food safety, aimed at the removal of citrinin from *Monascus* suspensions.

2. Materials and methods

Chemicals were purchased at the highest commercially available purity and were used without further treatment. Citrinin, iron(III) chloride hexahydrate (97%), sodium borohydride ($NaBH_4$), tetramethylammonium hydroxide, perchloric acid, ammonia solution (35% in water) were form Sigma–Aldrich, Italy.

2.1. Instrumentation

Optical and fluorescence measurements were performed in 1 cm quartz cuvettes using a Cary 50 spectrophotometer and a Cary Eclipse fluorescence spectrometer (Varian Inc., Palo Alto, CA, USA), respectively.

Transmission electron microscope (TEM) images were acquired by a JEOL 2010 microscope (JEOL Ltd., Tokyo, Japan), operating at 200 kV with a point-to-point resolution of 1.9 Å. The ^{57}Fe zero-field Mössbauer spectra were recorded at 300 K, employing a MS2007 (RCPTM, Czech Republic) Mössbauer spectrometer (Pechousek, Jancik, Frydrych, Navarik, & Novak, 2012), operating in a constant acceleration mode and equipped with a 50 mCi ^{57}Co(Rh) source. The values of isomer shift were referred to the metallic iron (α-Fe) at room temperature. The acquired Mössbauer spectra were fitted by the Lorentzian line shapes using the least-square method in the MossWin software program (Klencsár, Kuzmann, & Vértes, 1996).

A superconducting quantum interference device (SQUID, MPMS XL-7, Quantum Design) was used for the magnetization measurements. The hysteresis loops were recorded at a temperature of 300 and 5 K and in externally magnetic fields ranging from −5 to +5 T. The zero-field-cooled (ZFC) and field-cooled (FC) magnetization curves were recorded in a sweep mode of 1.8 K min^{-1}. The ZFC curve was measured after cooling the sample from 300 to 5 K in a zero magnetic field and the measurement was carried out on warming from 5 to 300 K under the external magnetic field (0.1 T). In the case of FC curve, similar process was employed, but the sample was cooled in an external magnetic field (0.1 T).

A series of Nd–Fe–B magnets (N35, 263–287 kJ m^{-3} BH, 1170–1210 mT flux density by Powermagnet – Germany) was used for the magnetic driving of nanoparticles.

2.2. Microorganism cultures

Monascus spp. (native strain DDJ 012010) and *Monascus purpureus* (native albino strain DDJ 032008) were obtained from the culture collection of the Federal University of Santa Catarina (UFSC, SC, Brazil). *Monascus ruber* (strain CCT 3802) was obtained from the Tropical Culture Collection André Tosello (Campinas—SP, Brazil). Strain spore suspensions were frozen at −20 °C after adding 100 μL glycerol mL^{-1} as a cryoprotector and stored for 3 months.

The inoculum and cultures were prepared in rice medium (20 g L^{-1} rice, 5 g L^{-1} glycine and 20 g L^{-1} agar-agar), pH 5.5. *Monascus* was initially grown on rice medium in a Petri dish at 30 °C for 7 days and subsequently stored at 4 °C. A spore suspension was obtained by washing the Petri dish cultures with a sterile aqueous solution of 0.1% Tween 80 (Vendruscolo, Ribeiro, Espósito, & Ninow, 2009).

One milliliter of this spore containing solution was mixed with 1 mL of semisolid agar (0.2% w/v)), and this suspension was used for one-point inoculation on Petri dishes, containing rice medium (25 mL) or rice medium containing 1 g L^{-1} SAMN. Plates were incubated at 25 °C for 12 days. Radial growth of *Monascus* spp. on Petri dishes was measured by a caliper every 12 h and the growth was followed for 12 days.

2.3. Synthesis of surface active magnetic nanoparticles

A typical synthesis of nanoparticles was already described (Magro & Faralli et al., 2012; Magro et al., 2012; Magro and Sinigaglia et al., 2012) and can be summarized as follows: $FeCl_3 \cdot 6H_2O$ (10.0 g, 37 mmol) was dissolved in MilliQ grade water (800 mL) under vigorous stirring at room temperature. $NaBH_4$ solution (2 g, 53 mmol) in ammonia (3.5%, 100 mL, 4.86 mol mol^{-1} Fe) was quickly added to the mixture. Soon after the reduction

reaction occurrence, the temperature of the system was increased to 100 °C and kept constant for 2 h. Then, the material was cooled at room temperature and aged in water, as prepared, for other 24 h. This product was separated by imposition of an external magnet and washed several times with water. This material can be transformed into a red brown powder (final synthesis product) by drying and curing at 400 °C for 2 h. The resulting nanopowder showed a magnetic response upon exposure to a magnetic field. The final mass of the product was 2.0 g (12.5 mmol) as Fe_2O_3 and a yield of 68% was calculated.

The nanoparticulated resulting material was characterized by Mössbauer and FT-IR spectroscopy, high resolution transmission electron microscopy, magnetization measurements and resulted constituted of stoichiometric maghemite (γ-Fe_2O_3) with a mean diameter (d_{avg}) of 11 ± 2 nm, which can lead to the formation, upon ultrasound application in water (Bransonic, mod. 221, 48 kHz, 50 W) of a stable colloidal suspension, without any organic or inorganic coating or derivatization.

3. Results and discussion

Citrinin presents a carboxylic and phenolic group (see Fig. 1). Thus, it can be considered a good candidate for chelating transition metals. Moreover, the ability of citrinin to chelate iron(III) in aqueous solutions was demonstrated by Da Lozzo et al. (2002). Therefore, considering the availability and reactivity of undercoordinate iron(III) sites on SAMN surface, (Magro & Baratella et al., 2014; Magro et al., 2014) these nanoparticles were exploited for citrinin recognition and binding.

3.1. Monascus cultures

It is well known that *Monascus* produces different pigments, yellow, orange and red in color Meinicke et al., 2012). From a chemical viewpoint, orange pigment is due to monascorubrin ($C_{23}H_{26}O_5$) or rubropunctatin ($C_{21}H_{22}O_5$), which are biosynthetized via trans-etherification of a hexaketide chromophore, produced by a polyketide synthase, with a molecule of a medium chain fatty acid. The yellow pigment is due to ankaflavin ($C_{23}H_{30}O_5$) and monascin ($C_{21}H_{26}O_5$), derived from the oxidation of the orange pigments, monascorubrin and rubropunctamine, respectively. Finally, red dyes, monascorubramine ($C_{23}H_{27}NO_4$) and rubropunctamine ($C_{21}H_{23}NO_4$), are produced by the reaction of the orange pigments with $-NH_2$ containing compounds (Dufossé et al., 2005; Hajjaj et al., 2012; Jung, Kim, & Shin, 2005; Kim, Jung, Kim, & Shin, 2006). Moreover, the final color of *Monascus* pigments greatly depends on the amino acid or protein with which the pigment is associated (Carvalho, Oishi, Pandey, & Soccol, 2005).

In the current work, 1.0 g L^{-1} suspensions of three different species of *Monascus*, namely *Monascus* spp., *M. ruber* and *M. purpureus* were cultured and characterized by UV–Vis and fluorescence spectroscopy. Noteworthy, the comparison of optical spectra indicated a higher dye production in the case of *Monascus* spp., and the presence of three spectral features at 270 nm, 380 nm, 490 nm, was observed (see Fig. 2). Pigments, yellow, orange and red, can be distinguished during low pressure chromatographic separations (see Fig. 2, inset). Moreover, *Monascus* suspensions were characterized

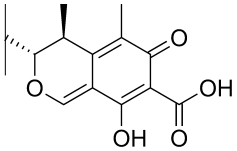

Fig. 1. Citrinin structure.

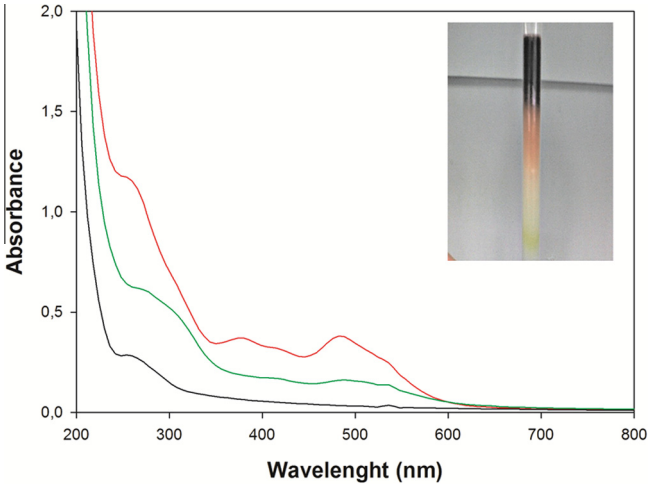

Fig. 2. Optical spectra of *Monascus* spp. (red), *Monascus purpureus* (black), *Monascus ruber* (green). Inset. low pressure chromatographic separation profile of *Monascus spp*. (For interpretation of the references to colour in this figure legend, the reader is referred to the web version of this article.)

by fluorescence spectroscopy. Only *Monascus* spp. samples, excited at 330 nm, led to an emission peak at around 500 nm, while samples of *M. purpureus* and *M. ruber* emitted at about 485 nm (see Fig. 3).

In agreement with literature reports (Zhou et al., 2012) excitation at 330 nm and emission at 500 nm can be attributed to citrinin. As a control, commercially available citrinin was studied by fluorescence spectroscopy, showing spectral features superimposable with *Monascus* spp. suspensions (see Fig. 3), thus evidencing a high mycotoxin production in this specie. By comparison with fluorescence spectra of known concentrations of pure citrinin, an estimate citrinin production of about 6.0 mg g^{-1} in *Monascus* spp., was calculated. Thus, if *Monascus* spp. represents a promising source of natural dyes, its high production of citrinin could hinder its real exploitation in food industry.

3.2. Analysis of Monascus growth and dye production in the presence of SAMNs

In order to observe the biological effect of SAMNs on *Monascus* spp., a method adapted from Donini, Bernardi, Minotto, and

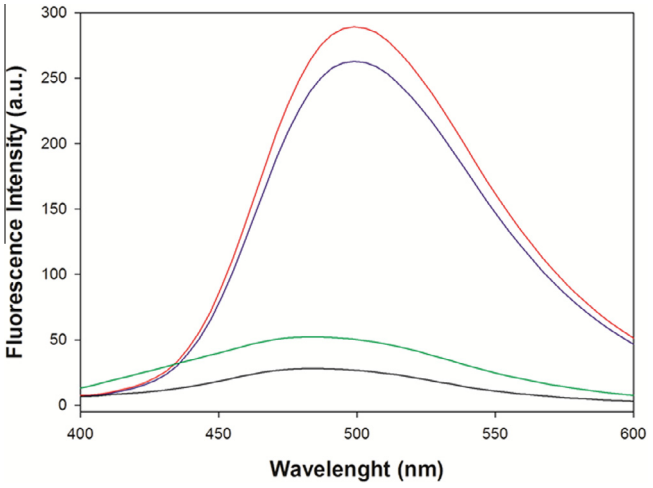

Fig. 3. Fluorescence spectra of *Monascus* spp. (red), commercial citrinin (blue), *Monascus purpureus* (black), *Monascus ruber* (green). (For interpretation of the references to colour in this figure legend, the reader is referred to the web version of this article.)

Nascimento (2006) was used, and fungal growth in the absence and in the presence of 500 mg L^{-1} nanoparticles was compared. According to Carvalho et al. (2005), a spore suspension was obtained by washing Petri dish cultures with a sterile aqueous solution of 0.1% Tween 80. Subsequently, aliquots (1 mL) were inoculated on Petri dishes containing of 20 g L^{-1} rice, 20 g L^{-1} agar and 5 g L^{-1} glycine (25 mL). Radial growth of *Monascus* spp. on Petri dishes was measured by a caliper every 12 h and the growth was followed for 12 days. Measurements were carried out from the center of the disk to the periphery of the colony (six measurements for each plate, four plates). Time (hours) and average radial growth measurements (mm) are reported in Fig. 4. As shown, growth rates of *Monascus* spp. in the absence and in the presence of SAMNs were superimposable, indicating no nanoparticle effect on fungal growth. Average radial growth rates for *Monascus* spp. in the absence and in the presence of SAMNs were 1.99 and 2.07 mm day^{-1}, respectively (see the inset of Fig. 4).

The effect of SAMNs on dye production by *Monascus* spp. (1 g L^{-1} suspensions) was studied by UV–Vis spectroscopy, in the SAMN concentration range comprised between 0.25 and 5 g L^{-1}. Spectral features of *Monascus* spp. in suspension were negligibly affected by the presence of SAMNs. We concluded that the presence of SAMNs did not deprive natural dyes from *Monascus* spp. suspensions, and these nanoparticles are suitable for the scope of the present study.

3.3. Application of SAMNs for citrinin removal

As above mentioned, SAMN surface exposes under-coordinated iron(III) sites, which are available for complex formation. Thus, SAMNs can be exploited for sequestrating iron chelating compound, such as citrinin, as this mycotoxin was already demonstrated to bind iron(III) in solution (Da Lozzo et al., 2002).

Preliminary, optical and fluorescence characteristics of citrinin were studied. Citrinin solutions show an optical spectrum with a shoulder at 250 and a band at 330 nm, characterized by extinction coefficients of ε_{250} = 9230 $M^{-1}cm^{-1}$ and ε_{330} = 4140 $M^{-1}cm^{-1}$ (see Supplementary Fig. S1 in Supplementary data), in good agreement with literature (Hackbart, Prietto, Primel, Garda-Buffon, & Badiale-Furlong, 2012). The fluorescence spectrum of citrinin presents its optimal excitation wavelength at 330 nm, and an emission band at 500 nm (see Fig. 3). Citrinin was stable for several days under our experimental conditions, and stock solutions in ethanol were stable for at least six months at −20 °C (see Supplementary Fig. S2 in Supplementary data).

In order to avoid possible optical interferences at short wavelength, the absorbance at 330 nm was chosen for the determination of citrinin concentration in solution. Citrinin bound on nanoparticles was calculated by difference with respect to its concentration in the supernatants.

When naked SAMNs were introduced in an aqueous solution containing citrinin, a complex, namely SAMN@citrinin, was

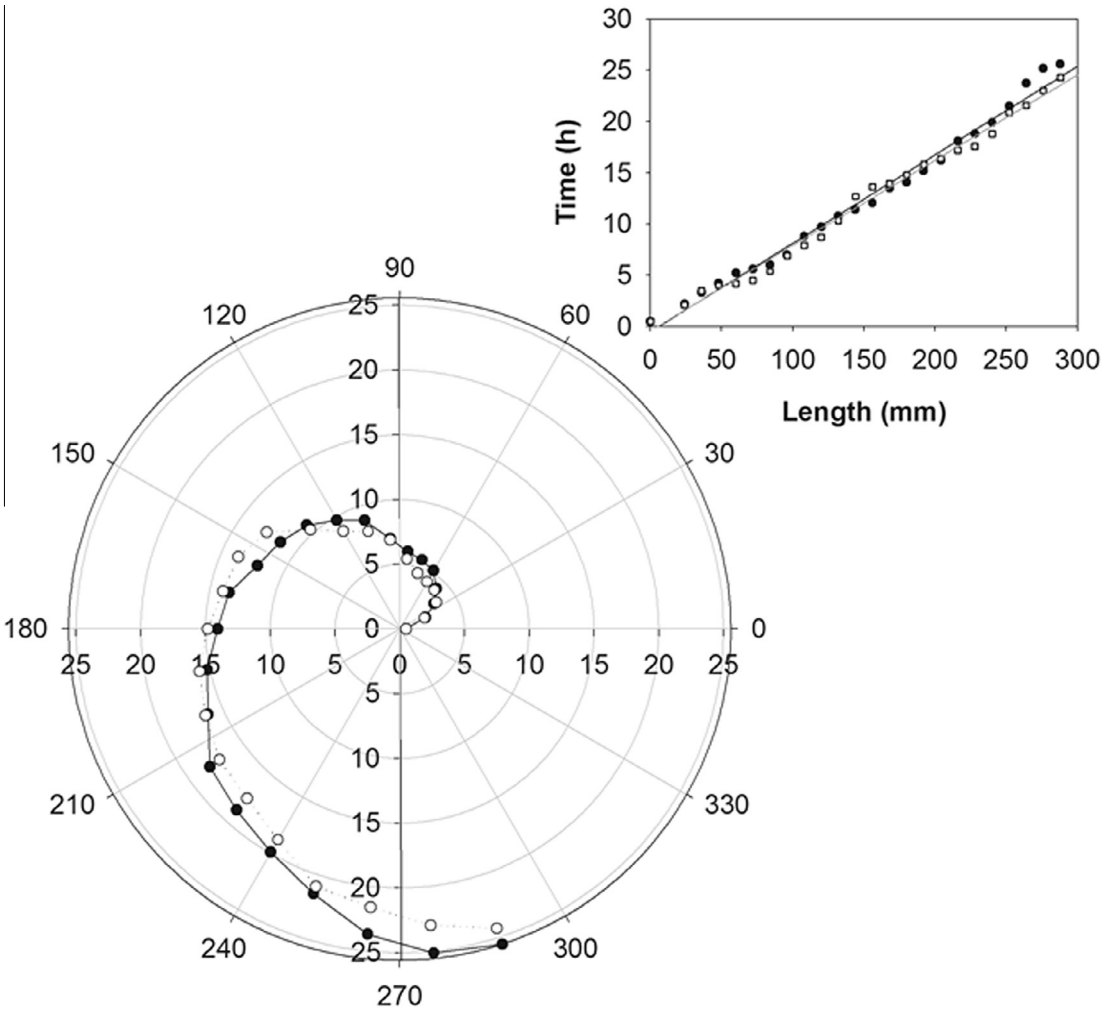

Fig. 4. Radial growth of *Monascus spp*. Inset: Radial growth rates in the absence and in the presence of 500 mg L^{-1} SAMN.

formed. SAMN@citrinin conjugate was magnetically isolated and washed several times with water. Mycotoxin coverage on SAMNs was stable, without any citrinin loss in solution, as checked by spectrophotometry.

The adsorption behaviour of citrinin was investigated in the SAMN concentration range comprised between 0.5 and 5.0 g L^{-1} and citrinin concentration range comprised between 6.25 mg L^{-1} and 0.25 g L^{-1}. According to the Langmuir model (Langmuir, 1918) we considered, as parameters characterizing the adsorption phenomenon, Γ as the surface concentration of bound citrinin when the bulk concentrations of the mycotoxin was [citrinin]. Thus, the surface fractional coverage can be calculated using the following saturation function (Hong, Lee, & Kim, 2005; Pisarchick & Thompson, 1990):

$$\theta = \frac{\Gamma}{\Gamma_{max}} = \frac{K\,[\text{citrinin}]}{1 + K\,[\text{citrinin}]}$$

Langmuir analysis assumes that each binding site on nanoparticle surface acts independently of other sites (Yang et al., 2003).

A saturation curve was obtained plotting Γ as function of [citrinin]. Interestingly, the amount of bound citrinin increased linearly without reaching a plateau. Moreover, the slope drastically changed at citrinin concentrations higher than 50 mg L^{-1}, leading to two different linear slopes in different citrinin concentration ranges (see Supplementary Fig. S3 in Supplementary data). For instance, at 1 g L^{-1} SAMNs, in the citrinin concentration range comprised between 6.25 and 50 mg L^{-1}, the percentage of SAMN bound citrinin, with respect [citrinin], was about 22%. Conversely, at citrinin concentrations higher than 50 mg L^{-1}, this value reached 96.0%. This peculiar behaviour suggests the occurrence of a cooperative phenomenon upon binding, observed at higher citrinin concentrations.

The classical Langmuir isotherm model has long been used as a first approach for the analysis, for example, of protein adsorption on ion-exchange, affinity, and IMAC sorbents (Belew, Yip, Andersson, & Porath, 1987). Nevertheless, some researchers noticed significant deviations from classical Langmuir behaviour (Hutchens & Yip, 1990; Hutchens, Yip, & Porath, 1988; Todd, Johnson, & Arnold, 1994; Wirth, Unger, & Hearn, 1993). Hutchens and colleagues (Hutchens & Yip, 1990; Hutchens et al., 1988) demonstrated that the deviation from the Langmuir behaviour can be explained by Scatchard analysis on the basis of "cooperativity" among the binding sites. We applied the same approach for citrinin binding on SAMN surface. Scatchard analysis suggested that citrinin binding on SAMN surface fits very well with a Langmuir absorption model at low mycotoxin concentrations. Interestingly, this phenomenon depended also on SAMN concentration. For instance, the linearity of Scatchard plot was confirmed at SAMN concentrations lower than 1.0 g L^{-1}, while above this value citrinin absorption did not follow the typical Langmuir behaviour, even at low citrinin concentrations. At citrinin concentrations comprised between 6.25 and 50.0 mg L^{-1} and at SAMN concentration lower than 1 g L^{-1}, a linear plot of the experimentally determined $\theta - 1$ as a function of [citrinin] $- 1$, yielded a Γ_{max} of 70.0 mg g^{-1} and K value of 5.0 L g^{-1}.

3.4. Structural characterization of the SAMN@citrinin complex

The SAMN@citrinin complex, prepared from a solution containing 50.0 mg L^{-1} citrinin and 0.5 g L^{-1} SAMN, was studied by high resolution electron transmission microscopy (see Fig. 5). TEM microscopy images indicated the presence of an organic matrix, forming a shell of about 1.0 nm around iron oxide nanoparticles, characterized by a lower electron density, attributable to citrinin molecules layering on the SAMN surface. Furthermore, by a more accurate observation of the high resolution images, the organic shell seems to be constituted by a multiple layer. This conformation is in good agreement with previous absorption study, which suggested the occurrence of a cooperative phenomenon. The resulting SAMN@citrinin complex was extremely stable and, if stored at 4 °C, citrinin remained firmly bound to the iron oxide nanoparticle surface for at least 12 months.

Magnetic nanoparticles reliability represents a fundamental requirement for exploiting magnetic separation at industrial level. For the actual applicability, a nanomaterial should respond to magnetic and structural prerequisites. For citrinin removal, nanomaterial structural stability should be guaranteed, as its degradation may represent a hazard. It should be mentioned that often nanoparticle coatings are not sufficiently stable and they tend to be dispersed. It is obvious that nanomaterial degradation or its coating deterioration represent a drawback, as these phenomena compromise the contaminant binding capability of the material. At the same time, nanomaterials should preserve their magnetic properties after binding, to be easily controlled by an external magnet during the removal process.

Structural and magnetic properties of as-prepared SAMN@citrinin were investigated by zero-field and in-field magnetization measurements, and Mössbauer spectroscopy. In order to monitor the magnetic response of SAMN@citrinin, hysteresis loops at 5 and 300 K and ZFC/FC magnetization curves were acquired (see Supplementary Fig. S4 in Supplementary data). Hysteresis loop measured at 5 K (Supplementary Fig. S4, panel a in Supplementary data) revealed that the system is magnetically ordered, even at the lower external magnetic fields (from 2 to 5 T), because all magnetic moments were oriented in a parallel way (saturated curve). The profile of the hysteresis loop around the origin was symmetric, with standard values of remanence (~12.03 $Am^2\,kg^{-1}$), but with the significantly lower values of coercivity (~2.70 mT) in comparison with the values reported for nanoparticles system of γ-Fe_2O_3 (Tucek, Zboril, & Petridis, 2006). The sudden decrease in the value of coercivity can be caused by the presence of diamagnetic substance, thus it witness citrinin shell on SAMN surface. This fact is also encouraged by the lower values of saturation magnetization (~63.33 $Am^2\,kg^{-1}$, while for bulk γ-Fe_2O_3 saturation magnetization is ~85 $Am^2\,kg^{-1}$). The magnetization vs. applied field measurement recorded at room temperature did not show any sign of hysteresis (see Supplementary Fig. S4, panel b and Supplementary Table S1 in Supplementary data). This implies the fact that system was in a superparamagnetic state. Superparamagnetic behavior means that the spins of all the magnetic nanoparticles fluctuate between the orientations of easy axis of magnetization.

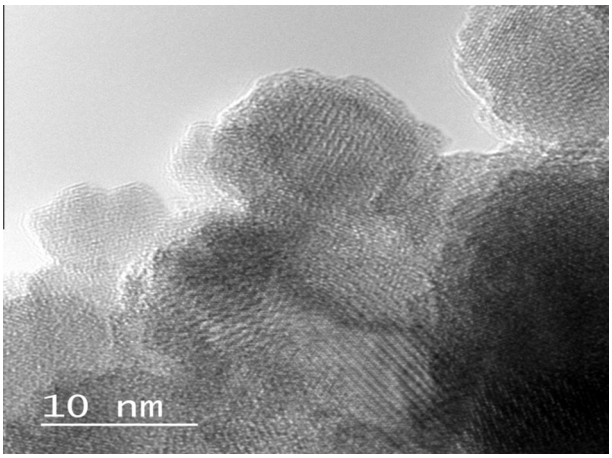

Fig. 5. TEM image of SAMN@citrinin complexes.

The phenomenon of the superparamagnetic behavior was confirmed by the ZFC/FC magnetization measurements (Supplementary Fig. S4, panel c in Supplementary data). When the temperature was decreased, the spins of all the magnetic nanoparticles subsequently freeze in the magnetically blocked regime. The temperature interval where the transition to the magnetically blocked state occurs is documented by a maximum at the ZFC magnetization curve and represents the blocking temperature (TB_{av}), at which the averaged size nanoparticles are magnetically blocked. In the SAMN@citrinin system, the blocking temperature was very close to ~54 K. The separation of two curves in ZFC/FC measurement is well known as the temperature of irreversibility (T_{irr}), which marks the onset of the blocking mechanism belonging to the largest nanoparticles in the system. In SAMN@citrinin system, T_{irr} was around ~176 K, which is far from the values of TB_{av}, suggesting a quite broad particles size distribution. In conclusion, magnetization characterization, witnessed the presence of citrinin on the surface of nanoparticles as a diamagnetic component, and, at the same time, confirmed that the hybrid material, SAMN@citrinin, still presents magnetic features suitable for magnetic separations.

Moreover, in-field Mössbauer spectroscopy was used, due to its unique ability to distinguish between structurally isomorphous maghemite and magnetite, to quantify the distribution of cations in tetrahedral an octahedral sites of these spinel structures, and to highlight modifications of nanoparticle crystal structure upon citrinin binding. The measured Mössbauer spectrum of the SAMN@citrinin sample is shown in Fig. 6 and values of the Mössbauer hyperfine parameters, derived from the spectrum fitting, are listed in Supplementary Table S2 in Supplementary data. At room temperature, the ^{57}Mössbauer spectrum can be fitted by one sextet component (see Fig. 6), with the Mössbauer hyperfine parameters listed in Supplementary Table S2 in Supplementary data. From the Mössbauer spectrum is clearly evident that the resonant lines of sextet component are not of Lorentzian character. Thus, to correctly fit the spectrum, a distribution of the hyperfine magnetic field (B_{hf}) was employed (see the inset in Fig. 6). The Mössbauer hyperfine parameters of the sextet component, well corresponding to the pure γ-Fe_2O_3, with Fe^{3+} ion in a high-spin state ($S = 5/2$) (Baikousi et al., 2012; Cornell & Schwertmann, 2004; Klencsár et al., 1996; Pechousek et al., 2012).

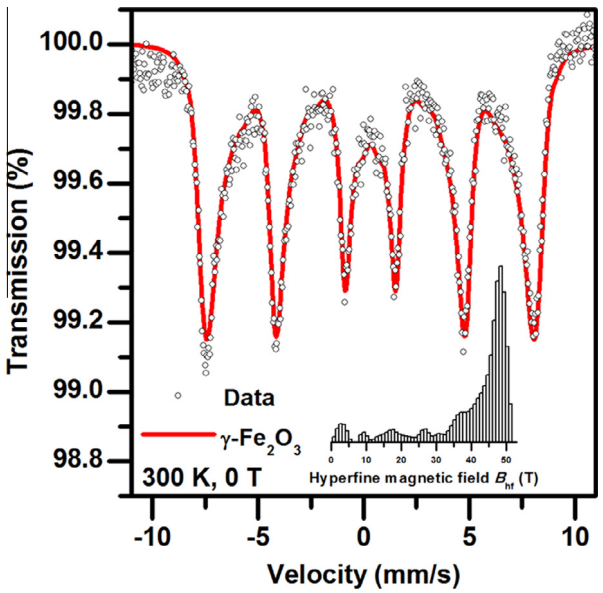

Fig. 6. ^{57}Fe Mössbauer spectrum of the SAMN@citrinin complex.

From the Mössbauer spectrum is also evident that no other spectral components corresponding to other iron valence state were detected, and/or that the citrinin substance does not significantly influenced Mössbauer parameters. Thus, we can conclude that SAMNs act as an excellent and stable magnetic carrier for citrinin, due to their well conserved magnetic and structural properties.

It should be reminded that hybrid nanoparticles (SAMN@citrinin) exhibited an excellent colloidal behavior with no indications of sedimentation and/or aggregation even within several days.

3.5. Magnetic removal of citrinin from Monascus cultures

In order to test the efficiency of SAMNs for citrin removal in a real sample, a 0.1 g L^{-1} *Monascus* spp. suspensions were treated with 1 g L^{-1} SAMNs. Previously, commercial citrinin was introduced in the fungal suspension (625 μg L^{-1}), to simulate a mycotoxin contamination, and its concentration was checked by HPLC using a fluorescence detector (excitation at 330 nm, emission at 500 nm) according to Vail and Homann (1990). Furthermore, this artificial contamination served as an internal control. Under these conditions, citrinin fluorescence signal was 196.0% higher with respect to the un-treated *Monascus* spp. suspensions. Contaminated *Monascus* suspensions were treated with 1 g L^{-1} SAMNs, leading to 70% citrinin removal. A second treatment, with the same nanoparticle amount, removed citrinin below the analytical detection limits (0.25 mg L^{-1}) (see Supplementary Fig. S5 in Supplementary data).

In conclusion, SAMNs stand out among other reported natural or synthetic nanomaterials, as they do not require any superficial modification or coating process to produce stable colloidal suspensions and their synthesis is completely carried out in water without any solvent. They present a high average magnetic moment and can be easily used to reversibly immobilize organic molecules (Magro & Faralli et al., 2012; Sinigaglia et al., 2012) and to develop biotechnological applications (Baratella et al., 2013; Magro et al., 2014; Venerando et al., 2013). Under-coordinated iron(III) sites on their surface can be used for complex formation reactions. Thus, as citrinin can form complexes with iron(III), its binding on SAMNs was exploited for mycotoxin removal from contaminated *Monascus* spp. cultures. In summary, SAMNs represent an efficient candidate for eliminating citrinin from *Monascus* spp. cultures for natural dye production, acting as an excellent and stable magnetic tool for applications in food industry.

Citrinin binding on SAMNs surface depends on the presence of a strong iron chelating feature on the toxin molecule, namely the keto-enol group. The strength of this binding was already illustrated in the case of curcumin by our group (Magro et al., 2014). The same chemical group can be found in dihydrocitrinone (DH-CIT) or in ochratoxin A (OTA). DH-CIT is a metabolite of citrinin DH-CIT, and, in humans, it can be considered as a detoxification step, characterized by a far lower toxicity than its precursor (Föllmann, Behm, & Degen, 2014). OTA is a well-known carcinogenic mycotoxin (Heussner & Bingle, 2015). Thus, if present in *Monascus* culture, the capture of dihydrocitrinone and OTA very likely occurs along with citrinin removal. Anyway, under our experimental conditions, only citrinin was found in *Monascus* cultures.

The proposed magnetic separation system, already proposed for the purification of curcumin from *Curcuma longa* rhizome extracts (Magro et al., 2015), and based on the specificity of iron binding properties of the molecule of interest, represents a promising alternative to conventional large scale purification or elimination of substances from food matrices.

Acknowledgments

Authors gratefully acknowledge CAPES (Brazil), process n. BEX 12199/13-3, University of Padua (Italy), grant "Assegni di Ricerca Junior" 2014 n. CPDR148959 and CARIPARO Foundation for the support. The work was supported by the Operational Program Research and Development for Innovations – European Regional Development Fund (CZ.1.05/2.1.00/03.0058). The authors acknowledge the support from the Ministry of Education, Youth and Sports of the Czech Republic (LO1305).

Appendix A. Supplementary data

Supplementary data associated with this article can be found, in the online version, at http://dx.doi.org/10.1016/j.foodchem.2016.01.147.

References

Baikousi, M., Bourlinos, A. B., Douvalis, A., Bakas, T., Anagnostopoulos, D. F., Tuček, J., ... Karakassides, M. A. (2012). Synthesis and characterization of γ-Fe_2O_3/carbon hybrids and their application in removal of hexavalent chromium ions from aqueous solutions. *Langmuir, 28*, 3918–3930.

Baratella, D., Magro, M., Sinigaglia, G., Zboril, R., Salviulo, G., & Vianello, F. (2013). A glucose biosensor based on surface active maghemite nanoparticles. *Biosensors & Bioelectronics, 45*, 13–18.

Belew, M., Yip, T. T., Andersson, L., & Porath, J. (1987). Interaction of proteins with immobilized Cu^{2+}: quantitation of adsorption capacity, adsorption isotherms and equilibrium constants by frontal analysis. *Journal of Chromatography, 403*, 197–206.

Carvalho, J. C., Oishi, B. O., Pandey, A., & Soccol, C. R. (2005). Biopigments from *Monascus*: Strain selection, citrinin production and color stability. *Brazilian Archives of Biology and Technology, 48*, 885–889.

Cornell, R. M., & Schwertmann, U. (2004). *The iron oxides: Structure, properties, reactions, occurrence and uses* (2nd ed.). Weinheim: Wiley-VCH Publishers.

Currall, S. C., King, E. B., Lane, N., Madera, J., & Turner, S. (2006). What drives public acceptance of nanotechnology? *Nature Nanotechnology, 1*, 153–155.

Da Lozzo, E. J., Mangrich, A. S., Rocha, M. E., De Oliveira, M. B., & Carnieri, E. G. (2002). Effects of citrinin on iron-redox cycle. *Cell Biochemistry and Function, 20*, 19–29.

Da Lozzo, E. J., Oliveira, M. B., & Carnieri, E. G. (1998). Citrinin-induced mitochondrial permeability transition. *Journal of Biochemical and Molecular Toxicology, 12*, 291–297.

Donini, L. P., Bernardi, E., Minotto, E., & Nascimento, J. S. (2006). Efeito da suplementação com garelos no crescimento in vitro de pleorotus ostrestus em meios à base de capim-elefante (Pennisetum spp.). *Arquivos do Instituto Biológico, 73*, 303–309.

Dufossé, L., Galaup, P., Yaron, A., Arad, S. M., Blanc, P., Murthy, K. N. C., & Ravishankar, G. A. (2005). Microorganisms and microalgae as sources of pigments for food use: A scientific oddity or an industrial reality? *Trends in Food Science & Technology, 16*, 389–406.

European Food Safety Authority (2012). Scientific Opinion on the risks for public and animal health related to the presence of citrinin in food and feed. *EFSA Journal, 10*, 2605.

Föllmann, W., Behm, C., & Degen, G. H. (2014). Toxicity of the mycotoxin citrinin and its metabolite dihydrocitrinone and of mixtures of citrinin and ochratoxin A in vitro. *Archives of Toxicology, 88*, 1097–1107.

Hackbart, H. C. S., Prietto, L., Primel, E. G., Garda-Buffon, J., & Badiale-Furlong, E. (2012). Simultaneous extraction and detection of ochratoxin A and citrinin in rice. *Journal of the Brazilian Chemical Society, 23*, 103–109.

Hajjaj, H., François, J. M., Goma, G., & Blanc, P. J. (2012). Effect of amino acids on red pigments and citrinin production in *Monascus ruber*. *Journal of Food Science, 77*, M156–M159.

Heussner, A. H., & Bingle, L. E. (2015). Comparative ochratoxin toxicity: A review of the available data. *Toxins, 7*, 4253–4282.

Hoehler, D., Marquardt, R. R., McIntosh, A. R., & Xiao, H. (1996). Free radical generation as induced by ochratoxin A and its analogs in bacteria (*Bacillus brevis*). *Journal of Biological Chemistry, 271*, 27388–27394.

Hong, M. Y., Lee, D., & Kim, H. S. (2005). Kinetic and equilibrium binding analysis of protein-ligand interactions at poly(amidoamine) dendrimer monolayers. *Analytical Chemistry, 77*, 7326–7334.

Hutchens, T. W., & Yip, T. T. (1990). Protein interactions with immobilized transition metal ions: Quantitative evaluations of variations in affinity and binding capacity. *Analytical Biochemistry, 191*, 160–168.

Hutchens, T. W., Yip, T. T., & Porath, J. (1998). Protein interaction with immobilized ligands: Quantitative analyses of equilibrium partition data and comparison with analytical chromatographic approaches using immobilized metal affinity adsorbents. *Analytical Biochemistry, 170*, 168–182.

International Risk Governance Council (2009). Policy brief: Appropriate risk governance strategies for nanotechnology applications in food and cosmetics. http://www.irgc.org/IMG/pdf/irgc_nanotechnologies_food_and_cosmetics_policy_brief.pdf (accessed August 25, 2015).

Jung, H., Kim, C., & Shin, C. S. (2005). Enhanced photostability of Monascus pigments derived with various amino acids via fermentation. *Journal of Agricultural and Food Chemistry, 53*, 7108–7114.

Kim, C., Jung, H., Kim, Y. O., & Shin, C. S. (2006). Antimicrobial activities of amino acid derivatives of Monascus pigments. *FEMS Microbiology Letters, 264*, 117–124.

Klencsár, Z., Kuzmann, E., & Vértes, A. (1996). User-friendly software for Mössbauer spectrum analysis. *Journal of Radioanalytical and Nuclear Chemistry, 210*, 105–118.

Langmuir, I. (1918). The adsorption of gases on plane surfaces of glass, mica and platinum. *Journal of the American Chemical Society, 40*, 1361–1403.

Magro, M., Baratella, D., Jakubec, P., Zoppellaro, G., Tucek, J., Aparicio, C., ... Vianello, F. (2015). Triggering mechanism for DNA electrical conductivity: Reversible electron transfer between DNA and iron oxide nanoparticles. *Advanced Functional Materials, 25*, 1822–1831.

Magro, M., Baratella, D., Salviulo, G., Polakova, K., Zoppellaro, G., Tucek, J., ... Vianello, F. (2014). Core–shell hybrid nanomaterial based on Prussian blue and surface active maghemite nanoparticles as stable electrocatalyst. *Biosensors & Bioelectronics, 52*, 159–165.

Magro, M., Campos, R., Baratella, D., Ferreira, M. I., Bonaiuto, E., Corraducci, V., ... Vianello, F. (2015). Magnetic purification of curcumin from *Curcuma longa* rhizome by novel naked maghemite nanoparticles. *Journal of Agricultural and Food Chemistry, 63*, 912–920.

Magro, M., Campos, R., Baratella, D., Lima, G., Holà, K., Divoky, C., ... Vianello, F. (2014). A magnetically drivable nanovehicle for curcumin with antioxidant capacity and MRI relaxation properties. *Chemistry – A European Journal, 20*, 11913–11920.

Magro, M., Valle, G., Russo, U., Nodari, L., & Vianello, F. (2012). Maghemite nanoparticles and method for preparing thereof. World Pat. WO/2012/010200.

Magro, M., Faralli, A., Baratella, D., Bertipaglia, I., Giannetti, S., Salviulo, S., ... Vianello, F. (2012). Avidin functionalized maghemite nanoparticles and their application for recombinant human biotinyl-SERCA purification. *Langmuir, 28*, 15392–15401.

Magro, M., Sinigaglia, G., Nodari, L., Tucek, J., Polakova, K., Marusak, Z., ... Vianello, F. (2012). Charge binding of rhodamine derivative to OH-stabilized nanomaghemite: Universal nanocarrier for construction of magnetofluorescent biosensors. *Acta Biomaterialia, 8*, 2068–2076.

Mapari, S. A., Thrane, U., & Mey, A. S. (2010). Fungal polyketide azaphilone pigments as future natural food colorants? *Trends in Biotechnology, 28*, 300–307.

Meinicke, R. M., Vendruscolo, F., Moritz, D. E., Oliveira, D., Schmidell, W., Samohyl, R. W., & Ninow, J. L. (2012). Potential use of glycerol as substrate for the production of red pigments by *Monascus ruber* in submerged fermentation. *Biocatalysis and Agricultural Biotechnology, 1*, 238–242.

Pechousek, J., Jancik, D., Frydrych, J., Navarik, J., & Novak, P. (2012). Setup of Mossbauer spectrometers at RCPTM. In: J. Tuček, & L. Machala (Eds.), Mössbauer spectroscopy in materials science, AIP Conference Proceedings. New York: American Institute of Physics. (pp. 186–193).

Pisarchick, M. L., & Thompson, N. L. (1990). Binding of a monoclonal antibody and its Fab fragment to supported phospholipid monolayers measured by total internal reflection fluorescence microscopy. *Biophysical Journal, 58*, 1235–1249.

Ribeiro, S. M., Campello, A. P., Chagas, G. M., & Kluppel, M. L. (1998). Mechanism of citrinin-induced dysfunction of mitochondria. VI. Effect on iron-induced lipid peroxidation of rat liver mitochondria and microsomes. *Cell Biochemistry and Function, 16*, 15–20.

Ribeiro, S. M., Chagas, G. M., Campello, A. P., & Kluppel, M. L. (1997). Mechanism of citrinin-induced dysfunction of mitochondria. V. Effect on the homeostasis of the reactive oxygen species. *Cell Biochemistry and Function, 15*, 203–209.

Satterfield, T., Kandlikar, M., Beaudrie, C. E. H., Conti, J., & Harthorn, B. H. (2009). Anticipating the perceived risk of nanotechnologies. *Nature Nanotechnology, 4*, 752–758.

Siegrist, M., Keller, C., Kastenholz, H., Frey, S., & Wiek, A. (2007). Laypeople's and experts' perception of nanotechnology hazards. *Risk analysis: An official publication of the Society for Risk Analysis, 27*, 59–69.

Sinigaglia, G., Magro, M., Miotto, G., Cardillo, S., Agostinelli, E., Zboril, R., ... Vianello, F. (2012). Catalytically active bovine serum amine oxidase bound to fluorescent and magnetically drivable nanoparticles. *International Journal of Nanomedicine, 7*, 2249–2259.

Stormer, F. C., & Hoiby, E. A. (1996). Citrinin, ochratoxin A and iron. Possible implications for their biological function and induction of nephropathy. *Mycopathologia, 134*, 103–107.

Todd, R. J., Johnson, R. J., & Arnold, F. H. (1994). Multiple-site binding interactions in metal-affinity chromatography: I. Equilibrium binding of engineered histidine-containing cytochromes c. *Journal of Chromatography A, 662*, 13–26.

Tucek, J., Zboril, R., & Petridis, D. (2006). Maghemite nanoparticles by view of Mossbauer spectroscopy. *Journal for Nanoscience and Nanotechnology, 6*, 926–947.

Vail, R. B., & Homann, M. J. (1990). Rapid and sensitive detection of citrinin production during fungal fermentation using high-performance liquid chromatography. *Journal of Chromatography, 535*, 317–323.

Vendruscolo, F., Ribeiro, C. S., Espósito, E., & Ninow, J. L. (2009). Biological treatment of apple pomace and addition in diet for fish. *Revista Brasileira de Engenharia Agricola e Ambiental, 13*, 487–493.

Venerando, R., Miotto, G., Magro, M., Dallan, M., Baratella, D., Bonaiuto, E., ... Vianello, F. (2013). Magnetic nanoparticles with covalently bound self-assembled protein corona for advanced biomedical applications. *Journal of Physical Chemistry C, 117*, 20320–20331.

Wirth, H. J., Unger, K. K., & Hearn, M. T. W. (1993). Influence of ligand density on the properties of metal-chelate affinity supports. *Analytical Biochemistry, 208*, 16–25.

Xu, B., Jia, X., Gu, L., & Sung, C. (2006). Review on the qualitative and quantitative analysis of the mycotoxin citrinin. *Food Control, 17*, 271–285.

Yang, J., Swaminathan, C. P., Huang, Y., Guan, R., Cho, S., Kieke, M. C., ... Sundberg, E. J. (2003). Dissecting cooperative and additive binding energetics in the affinity maturation pathway of a protein–protein interface. *Journal of Biological Chemistry, 278*, 50412–50421.

Zhou, Y. X., Chen, J. B., Dong, L. N., Chen, F. S., Hu, D. J., & Wang, X. H. (2012). A study of fluorescence properties of citrinin in beta-cyclodextrin aqueous solution and different solvents. *Journal of Luminescence, 132*, 1437–1445.

Massimiliano Magro received the degree in Chemistry at the University of Padua (Italy) in 2003. Since 2004, he worked on the synthesis and characterization of metal oxide nanostructures, in the development of nanobiosensors and biotechnological applications of magnetic nanoparticles. He is currently Senior Research Scientist at the Department of Comparative Biomedicine and Food Science of the University of Padua (Italy).

Denise Esteves Moritz graduated in Pharmacy and Biochemistry at the Federal University of Santa Catarina (SC, Brazil), where she got the Master degree in Biotechnology and the PhD in Chemical Engineering. She spent her post-doc in nanotechnology at University of Padua (Italy). She is currently professor at the University of Southern Santa Catarina (SC, Brazil). She is experienced in Bioprocess Engineering, focusing on Nanotechnology and Microbiology.

Emanuela Bonaiuto got the degree in Chemistry and Pharmaceutical Technologies at the University of Padua (Italy) in 2002. In 2009 she obtained her PhD in Biochemistry and Biophysics at the same University. Since 2006 she worked on the kinetic characterization of enzymes, in particular of Amino Oxidases, and on polyamines. Since 2014, she worked on the characterization of metal oxide nanostructures, in the development of nanobiosensors and biotechnological applications of magnetic nanoparticles. She is currently research fellow at the Department of Comparative Biomedicine and Food Science of the University of Padua (Italy).

Davide Baratella, after the B.Sc. graduation in Health Biotechnologies and the M.Sc. degree in Pharmaceutical Biotechnologies at the University of Padua (Italy), is currently a fellow at the Department of Comparative Biomedicine and Food Science of the University of Padua.

Milo Terzo received the degree in Biological Science at the University of Padua (Italy) in 2010. He is currently a fellow at the Department of Comparative Biomedicine and Food Science of the University of Padua.

Petr Jakubec received his degree in Chemistry in 2009 at the Palacky University in Olomouc (Czech Republic). In 2013 he obtained his Ph.D. at the same university under the supervision of J. Hrbáč and he became a junior researcher in the electrochemical group at RCPTM (Regional Centre of Advanced Technologies and Materials) in Olomouc (Czech Republic). His current research interests are focused on the development of new sensors and biosensors for detection of important molecules such as neurotransmitters, antibiotics and pesticides.

Ondřej Malina got her B.Sc. degree in Radiological Assistant at the Faculty of Health Sciences and her M.Sc. in Nanotechnology, Faculty of Science at Palacky University in Olomouc (Czech Republic), where she received her Ph.D. in Applied Physics. At the moment she is Junior Researcher at the Regional Centre of Advanced Technologies and Materials, Palacky University in Olomouc (Czech Republic). Her research activities are focused on magnetism of nanosized iron oxide-based systems, magnetization and physical properties measurements (SQUID and PPMS), zero-field and in-field ^{57}Fe Mössbauer spectroscopy.

Klára Čépe got her B.Sc. and M.Sc. degrees in Mathematics and Physics at the Faculty of Science, at Palacky University in Olomouc (Czech Republic), where she received her Ph.D. in Physics. At the moment she is a junior researcher at Regional Centre of Advanced Technologies and Materials, Palacký University, Olomouc (Czech Republic). Her research activities deal with electron microscopy, STEM, and scanning microscopies (AFM, MFM, STM).

Glaucia Maria Falcao de Aragao got her degree in Food Engineering from Universidade Estadual de Campinas (SP, Brazil), as the Master degree in Food Science. She received the PhD in Biotechnological Processes at the Institut National Des Sciences Appliquées, INSA, Toulouse, France, followed by postdoctoral studies at the Department of Food Science, University of Massachusetts at Amherst, United States. She is professor at the Department of Chemical Engineering and Food Engineering at the Federal University of Santa Catarina (SC, Brazil). She is experienced in biotechnological processes, mainly in the production of polyhydroxyalkanoates by *Cupriavidus necator* and predictive microbiology applied to food science.

Radek Zboril, after finishing the PhD study (2000), he underwent several short-term stays, e.g., at University of Delaware and University of Tokyo. From 2010, he is a professor at the Palacky University in Olomouc and the general director of the Regional Centre of Advanced Technologies and Materials, RCPTM (www.rcptm.com), in Olomouc, Czech Republic. He is an active member of the board of the Technology Agency of the Czech Republic. In 2011, he was awarded by the Czech Republic's Minister of Education for extraordinary results achieved in the field of research, experimental development and innovations. Professor Zboril is the author and principal investigator of more than 50 national and international grant projects with the total support over 45 mil EUR and he is author and co-author of more than 275 papers with the total impact factor over 1000.

Fabio Vianello got the degree in Biological Sciences and PhD in Biophysics. He is professor of biophysics and biochemistry in the Department of Comparative Biomedicine and Food Science at the University of Padua (Italy). He is involved in nanobiotechnology research and in the development of nanobiosensors and in the application of magnetic nanoparticles. At the same time he is working on food analysis and he is the director of the Master Course in Food Quality and Safety at University of Padua, visiting professor in Food Biochemistry at the Sao Paulo State University, Brazil, and visiting scientist at the Regional Centre of Advanced Technologies and Materials, Department of Physical Chemistry, Palacky University in Olomouc, Czech Republic.